Turkish Journal of Electrical Engineering & Computer Sciences

http://journals.tubitak.gov.tr/elektrik/

Research Article

Turk J Elec Eng & Comp Sci
(2020) 28: 865 – 874

doi:10.3906/elk-1905-153

Design of a low pass filter using rhombus-shaped resonators with an analytical LC equivalent circuit

Mohsen HOOKARI, Saeed ROSHANI*, Sobhan ROSHANI
Department of Electrical Engineering, Kermanshah Branch, Islamic Azad University, Kermanshah, Iran

Received: 27.05.2019 • **Accepted/Published Online:** 05.12.2019 • **Final Version:** 28.03.2020

Abstract: In this paper, a new method is presented for the design of a low pass filter (LPF) based on an LC equivalent circuit. Firstly, new formulas are proposed to calculate an LC equivalent circuit of a rhombus-shaped resonator. Secondly, the transfer function and transmission zero of the rhombus-shaped resonator are extracted, based on the presented formulas. Then other rhombus-shaped resonators are designed, based on the extracted formulas. The proposed filter has a cut-off frequency with an attenuation level of 3 dB at 1.54 GHz. The obtained return loss and insertion loss in the pass band are 16 dB and 0.1 dB, respectively. The designed filter is fabricated on RT-5880 with 31 mil thickness.

Key words: Compact size, LC equivalent circuit, low pass filter, microstrip, rhombus-shaped resonator, wideband

1. Introduction

Filters with good features like compact size, insertion loss, return loss, wide stopband, and sharp roll-off play important roles in many RF/microwave applications. They are used to pass or suppress various frequencies. Filters are used to choose or limit the RF/microwave signals within assigned spectral confines. Microstrip LPFs are important passive devices for suppressing noise and undesirable signals in communication systems [1–6]. Emerging technologies, such as wireless communications, WCDMA, and other wideband applications continue to challenge RF/microwave filters with ever more accurate requirements such as higher performance, smaller size, lighter weight, ultrawide stopband, and lower cost [1]. Thereby, various studies have been published to achieve an LPF with the mentioned features [7–11]. A compact LPF with a wide stopband is proposed in Liu et al. [7] using hairpin structures and stepped impedance units. Using coupled rhombic stubs, a compact and high selective LPF with a wide stopband is presented in Zhang et al. [8]. In Xiao et al. [9], an LPF is presented, based on a modified complementary split-ring resonator. A new microstrip lowpass filter using coupled T-shaped, elliptical, and radial resonators with features like sharp roll-off and high suppression level in the stopband is presented in Karimi et al. [10]. In Mousavi et al. [11], a microstrip lowpass filter based on a bend structure with some excellent features such as compact size and high suppression level in the stopband is proposed. In Palandoken [12] a mathematical method like LC equivalent circuit is introduced to design filters. In the present paper, a new method is presented to calculate an LC equivalent circuit of a rhombus-shaped resonator. Several rhombus-shaped resonators are combined to design the presented lowpass filter. The proposed lowpass filter has a stopband bandwidth from 1.76 GHz to 17.6 GHz. The size of the simulated filter is 22 mm × 12.3 mm. The proposed LPF is designed for L-band applications [13].

*Correspondence: s_roshany@yahoo.com

2. Main resonator

The rhombus-shaped resonator is similar to a rectangular resonator. Both of them can generate a transmission zero with a high attenuation level. However, matching a rectangular resonator with another resonator that has an angle like triangular or a rhombus-shaped resonator is difficult. In the present paper, an LC equivalent circuit of a rhombus-shaped resonator is extracted based on a rectangular resonator. The novel formulas are presented for the first time. The formulas needed for calculating LC equivalent of a rectangular resonator are written in (1) and (2). The rectangular resonator can be equaled by two capacitors and an inductor [1].

$$L_S = \frac{1}{2\pi f} \times Z_S \times \sin\left(\frac{2\pi L}{\lambda_g}\right) \tag{1}$$

$$C_S = \frac{1}{2\pi f} \times \frac{1}{Z_S} \times \tan\left(\frac{\pi L}{\lambda_g}\right) \tag{2}$$

Trigonometric functions can be used to calculate the LC equivalent circuit of the rhombus-shaped resonator. In the rectangular resonator, the length and width of transmission lines are important to calculate the LC equivalent circuit based on equations (1) and (2). The structure of the rhombus-shaped resonator is shown in Figure 1. The electromagnetic (EM) simulation result of the rhombus-shaped resonator is illustrated in Figure 2. As can be seen, the presented resonator has a transmission zero at 4.2 GHz.

$$Length_{New} = \frac{Length}{2\cos\frac{\theta}{2}} \tag{3}$$

To calculate the LC equivalent circuit of the rhombus-shaped resonator, the formulas of the rectangular resonator, (1) and (2), are used. If the widths of the rhombus-shaped resonator and the rectangular resonator are assumed equal while their areas are also considered equal, then (3) will be calculated. Thus, new formulas to compute the LC equivalent circuit of the rhombus-shaped resonator are written in (4) and (5).

$$L_S = \frac{1}{2\pi f} \times Z_S \times \sin\left(\frac{\pi L}{\lambda_g \times \cos\frac{\theta}{2}}\right) \tag{4}$$

$$C_S = \frac{1}{2\pi f} \times \frac{1}{Z_S} \times \tan\left(\frac{\pi L}{2\lambda_g \times \cos\frac{\theta}{2}}\right) \tag{5}$$

As can be seen in Figure 1, the main resonator is formed by rhombus-shaped and rectangular structures. Thus, to calculate the LC equivalent circuit of the main resonator, equations (1)–(5) can be used, so that L1 and L2 are calculated by (1) and C1 is computed by (2). L3 and C3 are calculated by (4) and (5), respectively. Moreover, C2 can be obtained by the sum of (2) and (5). To have a physical insight into each element, L1, L2, and C1 are related to rectangular structures, while L3 and C3 correspond to rhombus-shaped structures. In addition, C2 is related to rhombus-shaped and rectangular structures. The extracted LC equivalent circuit of the main resonator is depicted in Figure 3. The EM simulation result and LC equivalent circuit simulation result of the rhombus-shaped resonator are displayed in Figure 4. The values of the LC equivalent circuit of the rhombus-shaped resonator are given in Table 1.

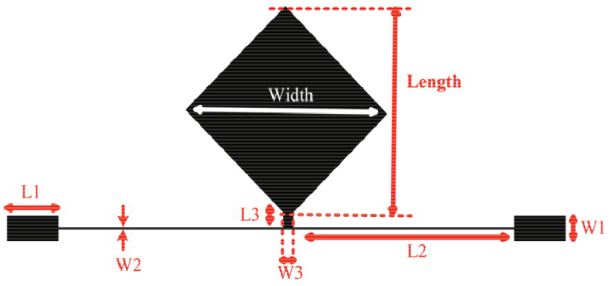

Figure 1. Rhombus-shaped resonator.

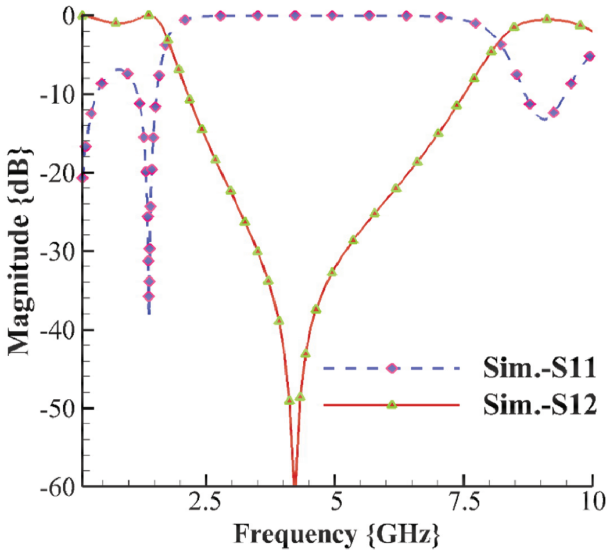

Figure 2. Frequency response of the rhombus-shaped resonator.

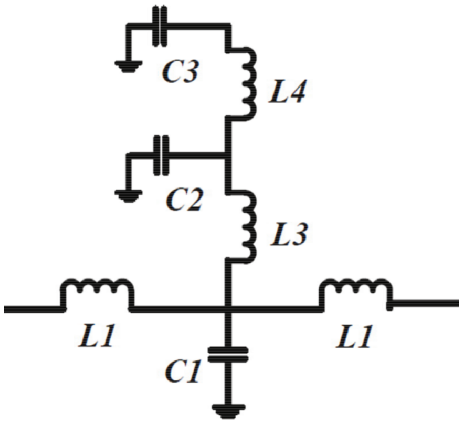

Figure 3. LC equivalent circuit of the rhombus-shaped resonator.

To perceive the effects of rhombus-shaped and rectangular structures on the transmission zero, the transfer function should be studied. The transfer function can be calculated by Kirchhoff's voltage law (KVL) and Kirchhoff's current law (KCL) rules. The transfer function of the main resonator is written in (6).

$$\frac{v_o}{v_i} = \frac{A_r}{(r + L_1S + L_2S)(2A + r + L_1S + L_2S)}, \tag{6}$$

where A is defined as follows:

$$A = \frac{S}{C3 + \frac{C_1+C_2+C_1C_2L_1S^2}{1+S^2(C_2L_2+C_1(L_1+L_2+C_2L_1L_2S^2))}} \tag{7}$$

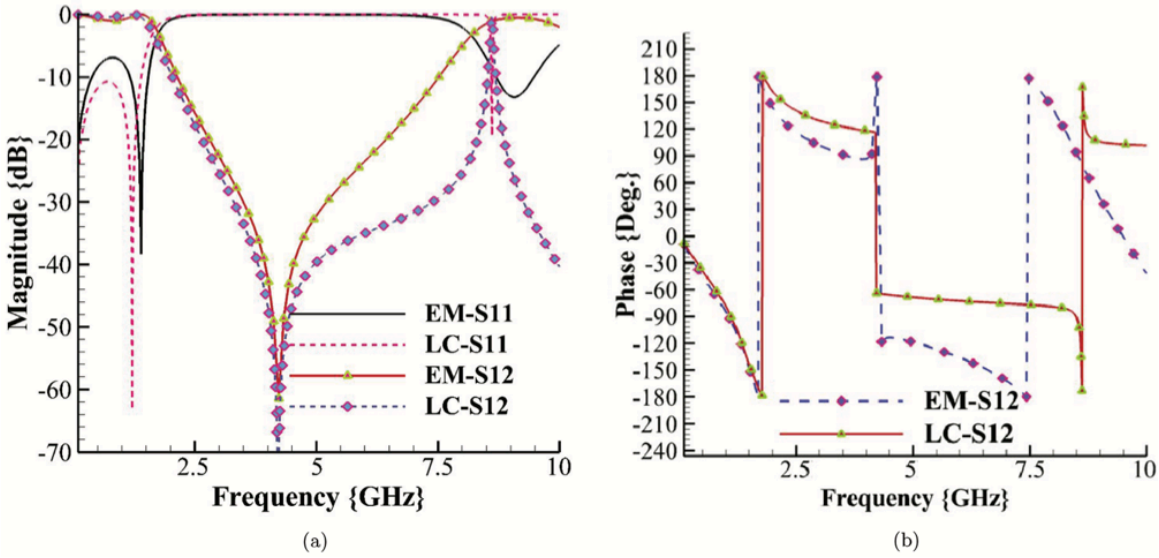

Figure 4. EM simulation result and LC equivalent circuit simulation result of rhombus shaped resonator, (a) magnitude and (b) phase.

Table 1. Calculated parameters of the LC equivalent circuit of the rhombus-shaped resonator.

Parameters	L1	L2	L3
Calculated	8.08 nH	0.43 nH	0.58 nH
Parameters	C1	C2	C3
Calculated	0.25 pF	0.94 pF	1.21 pF

The main resonator has a transmission zero at 4.4 GHz. The equation of transmission zero can be calculated by the obtained transfer function. Equation (8) shows the location of the other transmission zero. By using the equation of transmission zero a resonator can be presented with a controllable transmission zero, which is suitable for suppressing desirable frequency.

$$T_Z = \frac{\sqrt{-\frac{1}{C_1L_1} - \frac{1}{C_2L_1} - \frac{1}{C_2L_2} - \frac{\sqrt{-4C_1C_2L_1L_2+(C_1L_1+C_1L_2+C_2L_2)^2}}{C_1C_2L_1L_2}}}{\sqrt{2}} \tag{8}$$

L_2 is really effective in (8) and so the transmission zero frequency could be controlled by changing the L_2 value. L_2 corresponds to the main high impedance line of the resonator. Therefore, for decreasing the frequency of the transmission zero, this high impedance line length should be increased. Moreover, to increase the attenuation level of this transmission zero, two resonators can be added to the structure. The new resonator is shown in Figure 5. This new resonator has a transmission zero at 2 GHz. The frequency response of the new resonator is illustrated in Figure 6.

The LC equivalent circuit of the new resonator is calculated by (1)–(5), so that L1, L2, and L3 are calculated by (1) and C1 is computed by (2). L4 and C5 are calculated by (4) and (5), respectively. C4 can be obtained by the sum of (2) and (5). To have a physical insight into each element, L1, L2, L3, and C1 are related to rectangular structures and L4 and C5 correspond to rhombus-shaped structures. C4 is related

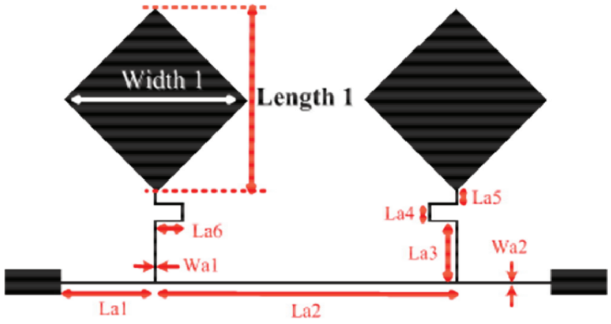

Figure 5. Structure of the double rhombus-shaped resonator.

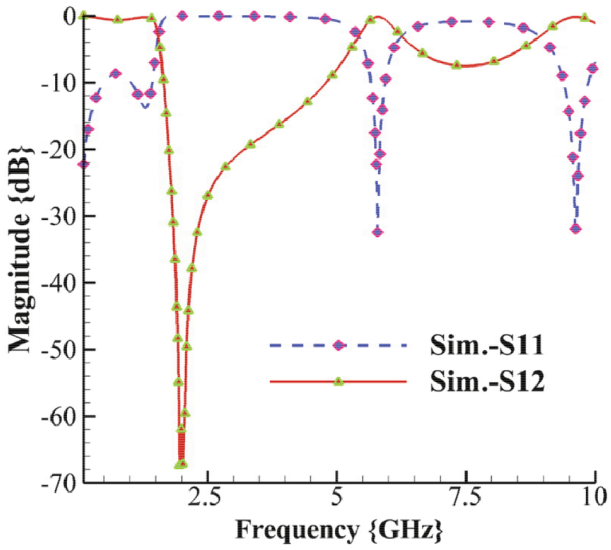

Figure 6. Frequency response of the double rhombus-shaped resonator.

to rhombus-shaped and rectangular structures. The double rhombus-shaped resonator is formed by rhombus-shaped and rectangular structures. The extracted LC equivalent circuit of the double rhombus-shaped resonator is depicted in Figure 7. The EM simulation result and LC equivalent circuit simulation result of the double rhombus-shaped resonator are displayed in Figure 8. The values of the LC equivalent circuit of the double rhombus-shaped resonator are given in Table 2.

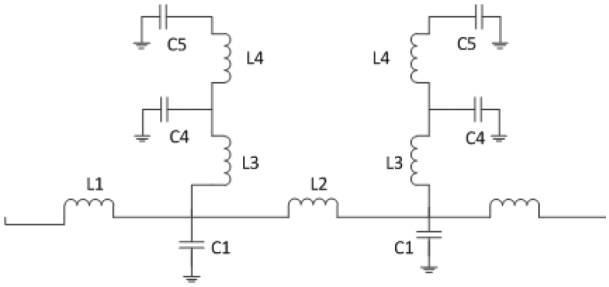

Figure 7. LC equivalent circuit of the double rhombus-shaped resonator.

The transfer function and transmission zero of the double rhombus-shaped resonator are extracted similar to the main resonator. They are written in (9) and (11), respectively.

$$\frac{v_o}{v_i} = \frac{ar}{(r + L_1S + L_2S + C_1L_2rS^2 + C_1L_1L_2S^3)\,(2a + r + L_1S + L_2S + 2aC_1rS + 2aC_1L_1S^2 + C_1L_2rS^2 + C_1L_1L_2S^3)} \tag{9}$$

$$a = \frac{\left(1 + C_4L_3S^2 + C_5L_3S^2 + C_5L_4S^2 + C_4C_5L_3L_4S^4\right)}{s\left(C_4 + C_5 + C_4C_5L_4S^2\right)} \tag{10}$$

$$T_Z = \frac{\sqrt{-\frac{1}{C_4L_3} - \frac{1}{C_4L_4} - \frac{1}{C_5L_4} - \frac{\sqrt{-4C_4C_5L_3L_4+(C_4L_3+C_5L_3+C_5L_4)^2}}{C_4C_5L_3L_4}}}{\sqrt{2}} \tag{11}$$

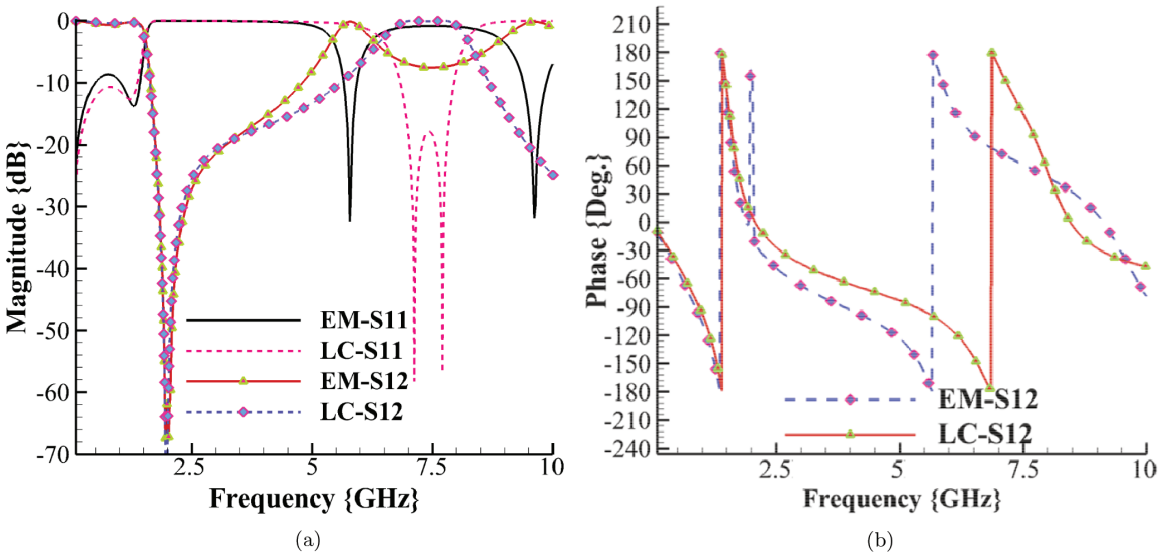

Figure 8. EM simulation result and LC equivalent circuit simulation result of the double rhombus-shaped resonator, (a) magnitude and (b) phase.

Table 2. Calculated parameters of LC equivalent circuit of double rhombus shaped resonator.

Parameters	L1	L2	L3	L4
Calculated	3.38 nH	10.3 nH	4.96 nH	0.74 nH
Parameters	C1	C2	C3	
Calculated	0.27 pF	1.1 pF	0.2 pF	

The main resonator and the double rhombus-shaped resonator cannot generate transmission zero at high frequencies (above 10 GHz). To generate a transmission zero at high frequencies, the capacitance and inductance values of the structure should be decreased. Thus, the dimensions of the new resonator have to be decreased. The new suppressor resonator and its frequency responses are displayed in Figures 9 and 10, respectively.

3. Low pass filter design

To design the final low pass filter, the examined rhombus-shaped resonators are combined in Figure 11. The presented filter generated several transmission zeros, but first and second transmission zeros are really important and so their equations were calculated in (8) and (11). The frequency response of the final filter is illustrated in Figure 12. The designed resonators generated three transmission zeros at 2, 4.4, and 11.5 GHz. However, the coupling structure between the resonators slightly changed the locations of the transmission zeros. In addition,

two new transmission zeroes at 9.1 GHz and 15.8 GHz were generated by the coupling effect between resonators in the final structure of the low pass filter, which can improve the stopband of the designed filter.

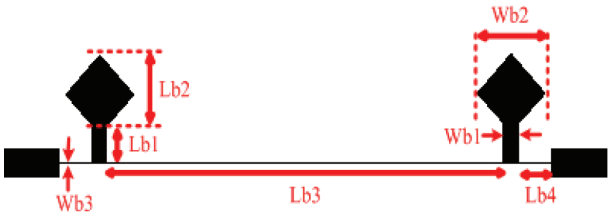

Figure 9. Suppressor cell structure based on rhombus-shaped resonators.

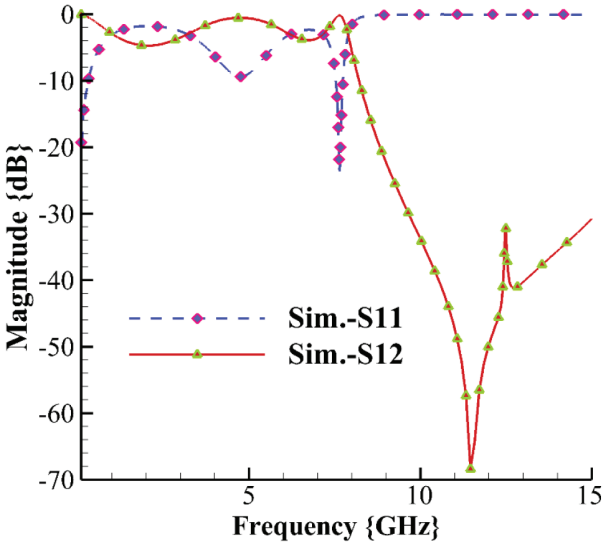

Figure 10. Frequency responses of the suppressor cell.

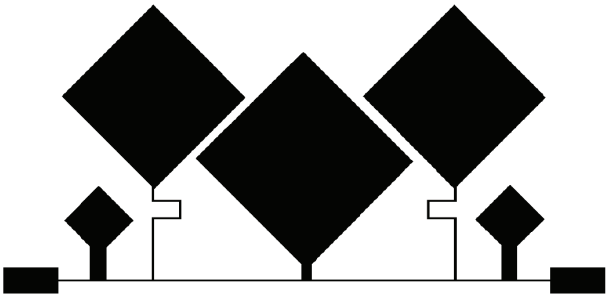

Figure 11. Layout of the final low pass filter.

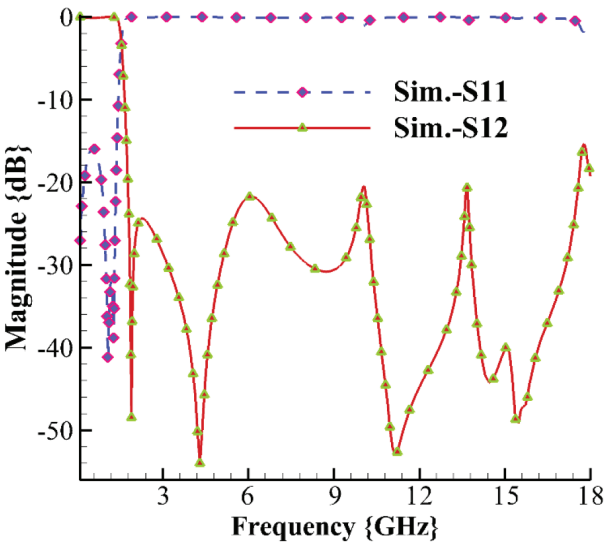

Figure 12. EM simulation results of the final low pass filter.

4. Simulation and experimental results

The lowpass filter is designed and fabricated on RT/Duroid 5880 substrate, with a relative dielectric constant of 2.2, thickness of 31 mil, and loss tangent of 0.0009. A photograph and S-parameters of the fabricated LPF are shown in Figures 13 and 14, respectively.

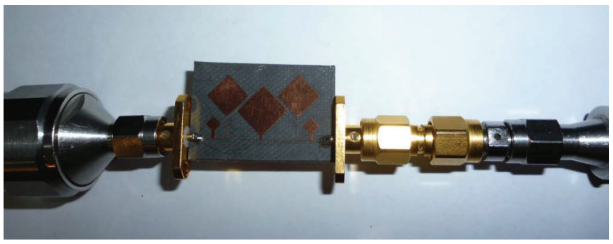

Figure 13. Photograph of the proposed LPF.

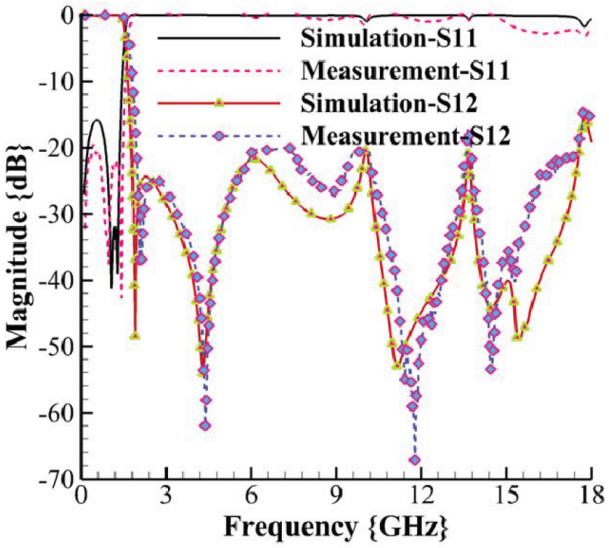

Figure 14. Measured and simulated results of the proposed LPF.

Table 3. Performance comparison between recent published filters and the proposed LPF.

Refs.	RO (ξ) (dB/GHz)	RSB	SF	NCS $\lambda_g \times \lambda_g$	FOM
[7]	52.8	1.52	2	0.081×0.113	17638
[8]	57.8	1.61	3.5	0.120×0.100	27142
[9]	188.8	0.92	2	0.200×0.180	9681
[14]	95	1.4	2	0.104×0.214	7388
[15]	75	1.66	2	0.107×0.083	28040
[16]	56.7	1.63	2	0.115×0.116	6928
[17]	74	1.74	2.4	0.090×0.136	25274
[18]	104	1.80	2.5	0.189×0.121	22510
[19]	57	1.19	4	0.180×0.240	6280
[20]	142	1.55	2.4	0.215×0.1	24,569
[21]	100	1.82	1.6	0.02	14,560
This work	123	1.6	2	0.080×0.140	35,780

The expansions for the table's parameters are as follows: RO = roll-off rate, RSB =relative stopband bandwidth, SF = suppression factor, NCS = normalized circuit size, and FOM = figure of merit.

The measured and simulation results are obtained by an Agilent network analyzer N5230A and EM-simulator Advanced Design System (ADS), respectively. The cut-off frequency of the proposed LPF is 1.54 GHz, while the stopband bandwidth is expanded from 1.76 GHz to 17.6 GHz with 20 dB attenuation level. The designed filter has a high figure of merit (FOM) equal to 35,780. For comparison, Table 3 shows a summary of key LPF performance metrics [11]. The group delay is shown in Figure 15. The result shows that group delay is really low. The designed lowpass filter has very good FOM in comparison other published articles.

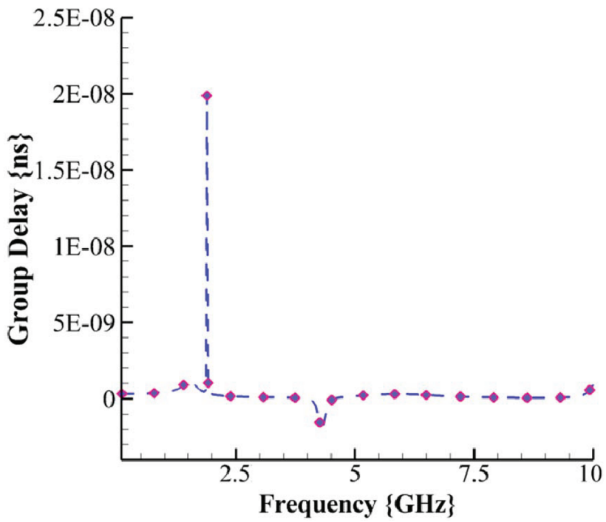

Figure 15. Group delay of the proposed LPF.

5. Conclusion

In this paper, a simple and compact microstrip LPF with an ultrawide stopband based on rhombus resonators is analyzed, designed, fabricated, and measured. The proposed filter has several desirable features, such as compact size, return loss better than –16 dB, and ultrawide stopband from 1.76 GHz to 17.6 GHz. With all these good features, the proposed LPF is recommended for modern communications systems.

References

[1] Hong JS, Lancaster MJ. Microstrip Filters for Rf/Microwave Applications. New York, NY, USA: Wiley, 2001.

[2] Pirasteh A, Roshani S, Roshani S. Compact microstrip lowpass filter with ultrasharp response using a square-loaded modified T-shaped resonator. Turkish Journal of Electrical Engineering & Computer Sciences 2018; 62 (4): 1736-1746.

[3] Roshani S, Golestanifar A, Ghaderi AH, Roshani S. Miniaturized LPF with sharp transition-band using semi-circle resonators. Applied Computational Electromagnetics Society Journal 2017; 32 (4): 344-351.

[4] Roshani S. A compact microstrip low-pass filter with ultra wide stopband using compact microstrip resonant cells. International Journal of Microwave and Wireless Technologies 2017; 9 (5): 1023-1027.

[5] Salehi A, Moloudian G, Setoudeh F. Design, simulation and manufacturing microstrip low-pass filter by wide stopband and changing fast situation from passing state to stopping. IETE Journal of Research 2018; doi: 10.1080/03772063.2018.1433079

[6] Tiwary AK, Gupta N. Performance of microstrip low-pass filter on electromagnetic band gap ground plane. IETE Journal of Research 2010; 56 (5): 230-234.

[7] Liu S, Xu J, Xu Z. Compact lowpass filter with wide stopband using stepped impedance hairpin units. Electronics Letters 2014; 51 (1): 1211-1214.

[8] Zhang B, Li SH, Huang J. Compact lowpass filter with wide stopband using coupled rhombic stubs. Electronics Letters 2015; 51 (3): 264–266.

[9] Xiao M, Sun G, Li X. A lowpass filter with compact size and sharp roll-off. IEEE Microwave and Wireless Components Letter 2015; 25 (120): 790-792.

[10] Karimi GH, Lotfi A, Siahkamari H. Design of microstrip lowpass filter with sharp roll-off using elliptical and radial resonators. Frequenz 2017; 71 (7): 349-356.

[11] Mousavi SMH, Makki SVAD, Siahkamari H. Design of microstrip lowpass filter using bend configuration with excellent sharpness in transition band. Frequenz 2016; 70 (5): 237-243.

[12] Palandoken M. Metamaterial-based compact filter design. In: Jiang XY (editor). Metamaterial, USA: IntechOpen, 2012.

[13] Pirasteh A, Roshani S, Roshani S. A modified class-F power amplifier with miniaturized harmonic control circuit. AEU-International Journal of Electronics and Communications 2018; 97: 202-209.

[14] Velidi VK, Sanyal S. Sharp roll-off lowpass filter with wide stopband using stub-loaded coupled-line hairpin unit. IEEE Microwave and Wireless Components Letters 2011; 21 (6): 301–303.

[15] Xu J, Ji YX, Wu W, Miao CH. Design of miniaturized microstrip LPF and wideband bpf with ultra-wide stopband. IEEE Microwave and Wireless Components Letter 2013; 23 (8): 397-399.

[16] Jiang S, Xu J. Compact microstrip lowpass filter with ultra-wide stopband based on dual-plane structure. Electronics Letters 2017; 53 (9): 607-609.

[17] Chen CHJ, Sung CHH, Su YD. A multi-stub lowpass filter. IEEE Microwave and Wireless Components Letter 2015; 25 (8): 532-534.

[18] Jiang SH, Xu J. Sharp roll-off planar lowpass filter with ultra-wide stopband up to 40 GHz. Electronics Letters 2017; 53 (11): 734-735.

[19] Li Q, Zhang Y, Li D, Xu K. Compact low-pass filters with deep and ultra-wide stopband using tri- and quad-mode resonators. IET Microwaves, Antennas & Propagation 2017; 11 (5): 743-748.

[20] Majidifar S, Ayati M. Design of a sharp response microstrip lowpass filter using taper loaded and radial stub resonators. Turkish Journal of Electrical Engineering & Computer Sciences 2017; 25 (5): 4013-4022.

[21] Majidifar S. High performance microstrip LPFs using dual taper loaded resonator. Optik-International Journal for Light and Electron Optics 2016; 127 (6): 3484-3488.